# Malaysian Journal of Analytical Sciences (MJAS)



**Published by Malaysian Analytical Sciences Society** 

# SYNTHESIS AND CHARACTERIZATION OF OXYGEN-DOPED MESOPOROUS GRAPHITIC CARBON NITRIDE USING NANODISC SILICA FROM RICE HUSK ASH AS HARD TEMPLATE

(Sintesis dan Pencirian Grafitik Karbon Nitrida Berliang Meso yang di Dop dengan Oksigen di Atas Nanocakera Silika dari Abu Sekam Padi Sebagai Templat Keras)

Shittu Fatimah Bukola<sup>1</sup>, Mohammad Anwar Mohamed Iqbal<sup>1</sup>\*, Farook Adam<sup>1</sup>, Mohamad Nasir Mohamad Ibrahim<sup>1</sup>, Nur Ruzaina Abdul Rahman<sup>2</sup>, Srimala Sreekantan<sup>2</sup>, Noor Hana Hanif Abu Bakar<sup>1</sup>, Mohd Hazwan Hussain Hussain, Hariy Pauzi<sup>3</sup>

<sup>1</sup>School of Chemical Sciences,
Universiti Sains Malaysia, 11800, Minden, Penang, Malaysia

<sup>2</sup>School of Materials and Mineral Resources Engineering

<sup>3</sup> Science and Engineering Research Centre (SERC)
Universiti Sains Malaysia, Engineering Campus, 14300 Nibong Tebal, Seberang Perai Selatan, Penang, Malaysia

\*Corresponding author: anwariqbal@usm.my

#### Abstract

Oxygen-doped mesoporous carbon nitride (O-MCN) was successfully synthesized through a polymerization reaction between urea and glucose using nanodisc silica (NDS) from rice husk ash as a hard template. The presence of oxygen within the framework of the MCN was confirmed using X-ray photoelectron spectroscopy (XPS) and Fourier-transformed infrared (FTIR) analyses. The scanning electron microscope (SEM) analysis indicates the existence of irregular spherical pores on the surface of O-MCN mimicking the surface morphology of the NDS. The Brunauer–Emmett–Teller (BET) surface area of the O-MCN (145  $m^2g^{-1}$ ) was similar to NDS (152  $m^2g^{-1}$ ). However, the Barrett, Joyner, and Halenda (BJH) pore size distribution of the O-MCN (48-84 Å) was smaller than the NDS (36-203 Å). The bandgap energy of the O-MCN was calculated to be 2.53 eV. The narrow bandgap energy suggests that the O-MCN has a high potential to be used as a photocatalyst under visible light irradiation.

Keywords: mesoporous carbon nitride, oxygen-doped mesoporous carbon nitride, rice husk, rice husk ash, photocatalyst

#### Abstrak

Karbon nitrida berliang meso mengandungi oksigen (O-MCN) berjaya disintesis melalui tindak balas pempolimeran antara urea dan glukosa menggunakan nanocakera silika (NDS) dari abu sekam padi sebagai templat keras. Kehadiran oksigen dalam kekisi MCN disahkan melalui analisis spektroskopi fotoelektron sinar-X (XPS) dan inframerah transformasi Fourier (FTIR). analisis mikroskop elektron imbasan (SEM) menunjukkan kewujudan liang sfera tidak sekata pada permukaan O-MCN yang menyerupai morfologi permukaan NDS. Luas permukaan Brunauer–Emmett–Teller (BET)O-MCN (145 m²g⁻¹) sama dengan NDS (152 m²g⁻¹). Walau bagaimanapun, taburan saiz liang Barrett, Joyner, and Halenda (BJH) O-MCN (48- 84 Å) adalah lebih kecil berbanding NDS (36-203 Å). Tenaga sela jalur O-MCN dikira sebagai 2.53 eV. Tenaga sela jalur yang sempit mencadangan O-MCN mempunyai potensi yang tinggi untuk digunakan sebagai fotokatalis dibawah iradiasi cahaya nampak.

**Kata kunci:** karbon nitrida berliang meso, karbon nitrida berliang meso mengandungi oksigen, sekam padi, abu sekam padi, fotopemangkin

#### Introduction

Carbon nitride (CN) is a polymeric material containing carbon and nitrogen atoms that has unique properties such as semi conductivity, basicity, high hardness, chemical robustness, high chemical and mechanical stability. These properties rely on the structure, composition, and crystallinity of the CN framework. So far, five different types of structures of CN have been reported. Namely, carbon nitrides  $C_3N_4$  (g- $C_3N_4$ ),  $\alpha$ - $C_3N_4$ , β-C<sub>3</sub>N<sub>4</sub>, cubic-C<sub>3</sub>N<sub>4</sub>, and pseudocubic-C<sub>3</sub>N<sub>4</sub>. The former is a two-dimensional CN, whereas the latter is threedimensional CNs. Among these CNs, g-C<sub>3</sub>N<sub>4</sub> has gotten considerable attention because of its unique and combined properties such as extreme hardness, energystorage capacity, semi conductivity, gas adsorption capacity, and low density [1]. However, low surface area (<10 m<sup>2</sup> g<sup>-1</sup>) and porosity hamper the application of g-C<sub>3</sub>N<sub>4</sub> in the area of adsorption and catalysis even though the presence of basic sites is considered beneficial [1].

Since the discovery of mesoporous carbon nitrides (MCN) by Vinu et al. in 2005, various types of MCN with large surface area, pore volume, and pore diameters have been synthesized. Larger surface area can support more active sites for reaction, whereas the porous structure can improve the light absorption [2, 3]. The MCNs have been synthesized using hard-templating (nanocasting or replication) and soft-templating (self-assembly) approaches. The MCNs synthesized *via* hard-templating approach indicate better control and replication of the morphology of the targeted product compared to the MCNs prepared *via* soft-templating approach [4].

Various types of oxygen doped mesoporous carbon nitrides (O-MCN) have been reported to be active as photocatalysts under visible light irradiation [5, 6]. Among the limitations concerning the synthesis strategies of O-MCN are the use of environmentally unfriendly C, N, and O precursors such as carbon tetrachloride, formaldehyde and ethylenediamine, and multiple synthesis steps. In addition, the silica

precursors used in the synthesis of the hard template are from commercial sources such as tetraethyl orthosilicate (TEOS).

In this paper, O-MCN was synthesized *via* hard templating method in a single step by polymerizing urea and glucose as the C, O, and N sources. Nanodisc silica (NDS) prepared from rice husk ash (RHA) was used as the hard template. The NDS produced from RHA add value to agricultural waste, particularly rice husk, it's environmentally advantageous, low cost of production and abundantly available. The physicochemical characterizations indicate that the catalysthas potential to be used as a photocatalyst. To the best of our knowledge, no reports were found on the use of NDS from RHA as a template for the synthesis of O-MCN.

#### **Materials and Methods**

#### Raw materials

Nitric acid (HNO<sub>3</sub>, 69%), sodium hydroxide (NaOH, , >99%), glucose ( $C_6H_{12}O_{6,}$  >99%), urea ( $CH_4N_2O$ , >99%) and hydrofluoric acid (HF, 49%, QREC). All chemicals were of analytical grade and used without further purification.

### Synthesis of rice husk ash

The RHA was produced from rice husk (RH) according to the method reported by Adam et al [7]. The rice husk was washed with plenty of water and then rinsed with distilled water to remove all the soluble dirt and soil. The RH was dried at room temperature for 48 hours. The clean and dried RH was then stirred in 750 mL (1.0 M) HNO<sub>3</sub> for 24 hours to reduce the metallic impurities. It was further washed thoroughly with distilled water until the pH of the filtrate reached 7. The acid-treated RH was dried for 24 hours at 110 °C and then pyrolyzed at 600 °C for 6 hours to remove the organic components of the RH in a furnace. A white colored RHA was obtained at the end of the process.

#### Synthesis of NDS

A sodium silicate solution was prepared by dissolving 5.0 g of the RHA in 500 mL (0.5 M) aqueous NaOH solution [8]. The pH of the sodium silicate solution was reduced to pH 7 by adding 2.0 M HNO<sub>3</sub> under vigorous stirring at 1200 rpm. The silica gel started to form when the pH of the sodium silicate reached 7. The gel was aged in the mother liquor for 24 hours in a closed plastic container under vigorous stirring and then for 48 hours under static to allow the silica gel to slowly precipitate. After the aging process, the formed gel was filtered and washed with distilled water until the pH of the filtrate became constant. The washed silica gel was freeze-dried to remove water [9]. A fine white powder of NDS was obtained. The powder was kept in a desiccator for further use.

#### **Synthesis of O-MCN**

The O-MCN was prepared using the method reported by Hu et al. [10] with some modifications. In a typical synthesis process, glucose (0.5 g) and urea (10 g) were dissolved in 100 mL of distilled water and heated to 70 °C under stirring. Into the solution, 0.3 g of NDS was added as a hard template. The solution was stirred at 80 °C until the water evaporated. The catalyst was then transferred into a 50 mL crucible and dried in the oven at 80 °C for 24 hours. The catalyst was uniformly ground and calcined at 550 °C for 1 hour at a heating rate of 5 °C min<sup>-1</sup>. A dark brown colored powder was obtained. The powder was then dispersed in 100 mL of an aqueous solution of HF overnight to remove the NDS [11]. The O-MCN powder was filtered and washed with 1000 mL distilled water, followed by drying at 80 °C overnight.

### Catalyst characterization

The prepared samples were characterized by FT-IR spectroscopy (Perkin Elmer System 2000 FT-IR Spectrophotometer) using KBr pellets technique, N<sub>2</sub> adsorption porosimetry (Micromeritics Instrument Corporation model ASAP 2000, Norcross), powder X-ray diffraction (Siemens Diffractometer D5000 diffractometer Kristalloflex, equipped with CuK radiation,= 0.154 nm), scanning electron microscopy (Leica Cambridge S360), energy dispersive spectrometry (EDAX FALCON SYSTEM), UV–Vis

diffuse reflectance spectroscopy (Perkin Elmer Lambda 35 UV–Vis spectrophotometer) and the XPS spectrum was recorded on AXIS Ultra DLD, Kratos, equipped with an AIK X-ray source = 1486.6 eV at 10 mA, 15 kV). All binding energies were calibrated using contaminant carbon (C 1 s = 284.6 eV) as reference. The C, N, and O content were determined using CHNO analyzer.

### **Results and Discussion**

#### **SEM** analysis

Figures 1 (a) and (b) represent the SEM image of NDS and O-MCN, respectively. From Figure 1(a), it can be seen that the surface of NDS is constructed of irregular spherical shaped nanoparticles. The de-templating of NDS from the framework of O-MCN using aqueous HF had created a porous surface, as shown in Fig. 2(b). The pores on the surface of O-MCN were spherically shaped with various sizes similar to the surface of NDS.

#### **HRTEM** analysis

The HRTEM images of NDS and O-MCN are shown in Figures 2(a) and (b). The HRTEM of NDS revealed disc-like particles with sizes in the range of 58 to 63 nm. The HRTEM of O-MCN (Figure 2(b)) indicates the interconnected elongated rod-like nanoparticles with undefined pore channels. Often, the MCN will replicate the hard template used in the synthesis process. The O-MCN synthesized by Park et al. [12] replicated the morphology of the hard templates, SBA-15, and cubic meso-SiO<sub>2</sub> that they had used. Cha et al. [13] synthesized sulphur doped MCN (S-MCN) utilizing SBA-15 as the hard template, and they too observed that the S-MCN replicated the SBA-15 as well. Surprisingly, in this research, the synthesized O-MCN did not replicate the disc-like morphology of the NDS. The replication was not observed, possibly due to the physical properties of the NDS compared to SBA-15 and O-MCN synthesis procedure. However, further investigations are required to confirm these assumptions.

#### Nitrogen sorption analysis

The nitrogen adsorption-desorption isotherms of the NDS and O-MCN is shown in Figure 3. Both materials

exhibit type-IV isotherm with H3 hysteresis loop. The type-IV isotherm confirm the existence of mesopores, whereas the H3 hysteresis loop indicates the mesopores are slit-shaped with non-uniform size [14]. The BET surface area of O-MCN (145 m $^2$ g $^{-1}$ ) is slightly lower compared to NDS (152 m $^2$ g $^{-1}$ ). The BJH pore size distribution determined from the adsorption branch is given in inset of Figure 4. From the porogram of NDS, the mesopore distribution was predominantly in the

range of 39-203 Å. The etching process using HF had created pores with broad diameter range. The pore size distribution in O-MCN was determined to be in the range of 48- 84 Å. The existence of pore sizes in a broad range is also visible, as in the SEM image of O-MCN (Figure 1(b). The pore volume of NDS was 0.30 cm<sup>3</sup>g<sup>-1</sup>, whereas the pore volume of O-MCN was 0.28 cm<sup>3</sup>g<sup>-1</sup>.

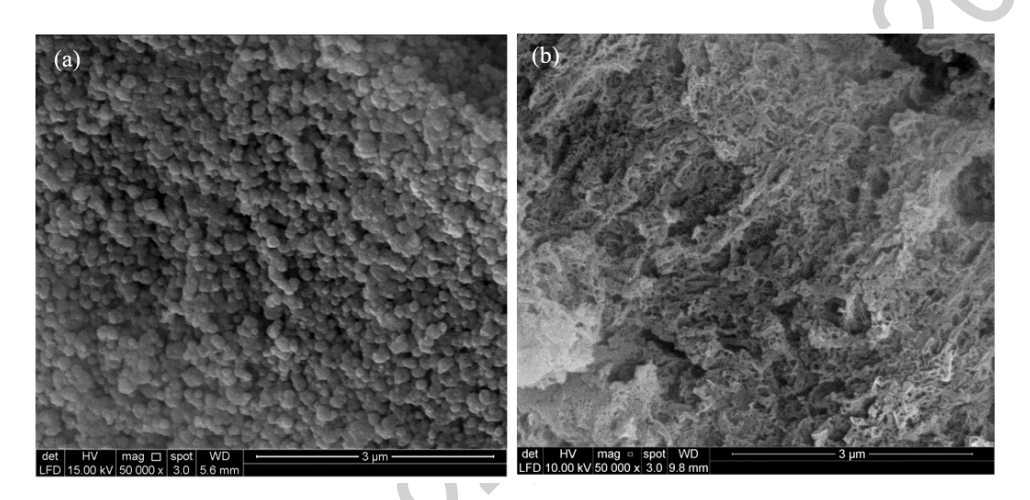


Figure 1. The SEM images of (a) NDS (magnification?) and (b) O-MCN

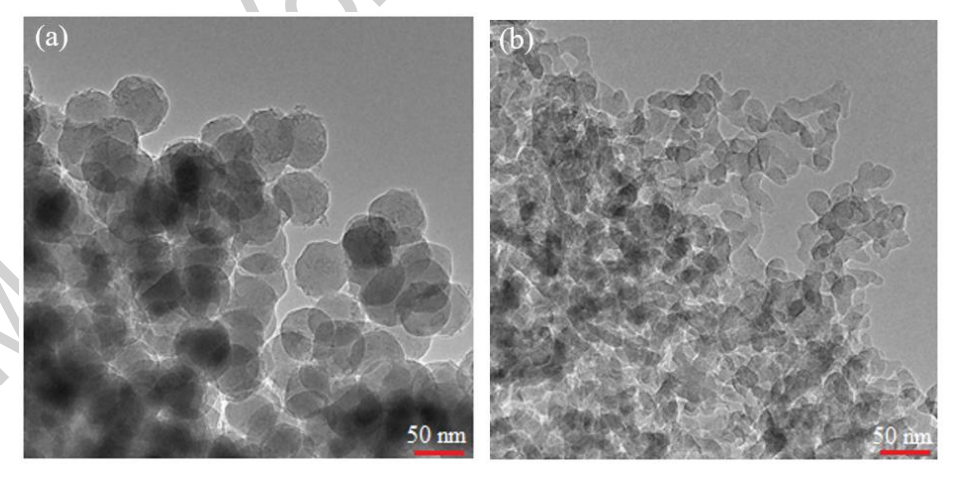


Figure 2. The HRTEM image of (a) NDS and (b) O-MCN

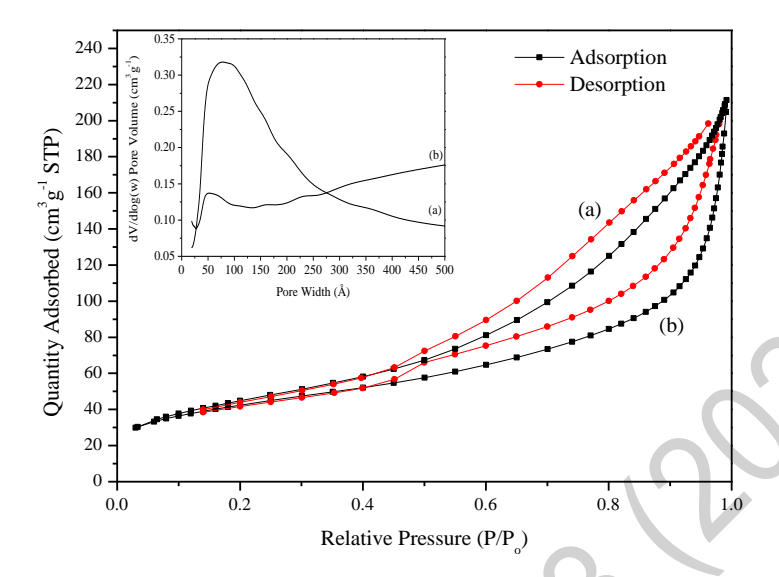


Figure 3. The nitrogen adsorption isotherms and BJH pore size distribution (inset) of (a) NDS and (b) O-MCN

# FT-IR analysis

The FT-IR spectrum of O-MCN is shown in Figure 4. The sharp intense band observed at 810 cm<sup>-1</sup> is assigned to the characteristic bending modes of triazine units [15]. The bands with weak intensity at 3159 and 3315 cm<sup>-1</sup> are assigned to the stretching modes of secondary and primary amines and their intermolecular hydrogen bonding [16]. The collection of bands at 1200-1600 cm<sup>-1</sup> is due to the stretching vibrations of heptazine-derived repeating units [17]. The absorption band at 2163 cm<sup>-1</sup> is assigned to C≡N or N=C= N due to incomplete polymerization of the precursors [18]. The presence of the C-O bond is indicated by the presence of a weak shoulder at 1156 cm<sup>-1</sup>. The IR bands related to the silica matrix could not be detected, indicating the successful removal of the template using aqueous HF.

#### X-ray diffraction analysis

The XRD pattern of the synthesized O-MCN is shown in Figure 5. A diffraction peak with a strong intensity at  $2\theta = 27.2^{\circ}$  in the diffractogram of the O-MCN is indexed to the (002) crystal plane. The plane is attributed to the lamellar packing of graphite in the  $\pi$ -conjugate plane [19]. The  $d_{002}$  value of O-MCN calculated from Bragg Equation was 0.329 nm. The

value was relatively shorter compared to pure graphitic carbon (0.353 nm) [20]. The crystallite size of O-MCN determined from the Scherrer Equation was 3.00 nm. The peak associated with amorphous silica at  $2\theta \sim 22^\circ$  is also invisible [21], indicating the high purity of O-MCN.

#### **CHNO** analysis

The elemental analysis of O-MCN is summarized in Table 1. The chemical composition of the O-MCN shows a C/N ratio of 0.75 which is equivalent to the ideal or theoretical C/N value (0.75) of single-crystalline graphitic carbon nitride [22].

#### X-ray photoelectron analysis

The XPS of C 1s spectrum (Figure 6(a)) was fitted into five peaks at 283.2, 284.6, 285.9, 286.8 and 288.1 eV. These are attributed to sp<sup>2</sup> hybridized graphitic carbon, sp<sup>3</sup> hybridized graphitic carbon, N-C=C bond, C-O and C=N/C=O bonds, respectively [23, 24]. The deconvolution of O 1s spectrum resulted in two peaks at 529.2 and 531.3 eV (Fig. 6(b)). The former peak corresponds to the lattice oxygen, whereas the latter corresponds to the presence of C-O functional group [25]. The deconvolution of N 1s spectrum shown in Figure

6(c) shows the existence of three peaks. The peak at 396.8 eV could be assigned to the sp<sup>2</sup> hybridized aromatic nitrogen bonded to carbon atoms (C-N=C) while the peak at 398.4 eV emerged from the tertiary nitrogen in the triazine units N-C<sub>3</sub> groups. Finally, the peak at 401.3 eV is derived from N atom

of the amino-functional group with H-atom (C-N-H) in the aromatic CN heterocycles [26, 27].

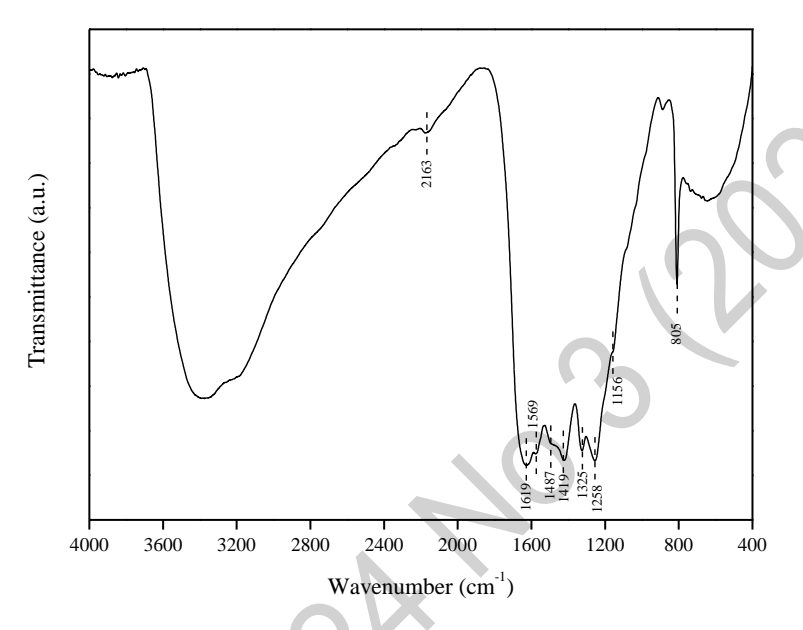


Figure 4. The FT-IR spectrum of O-MCN.

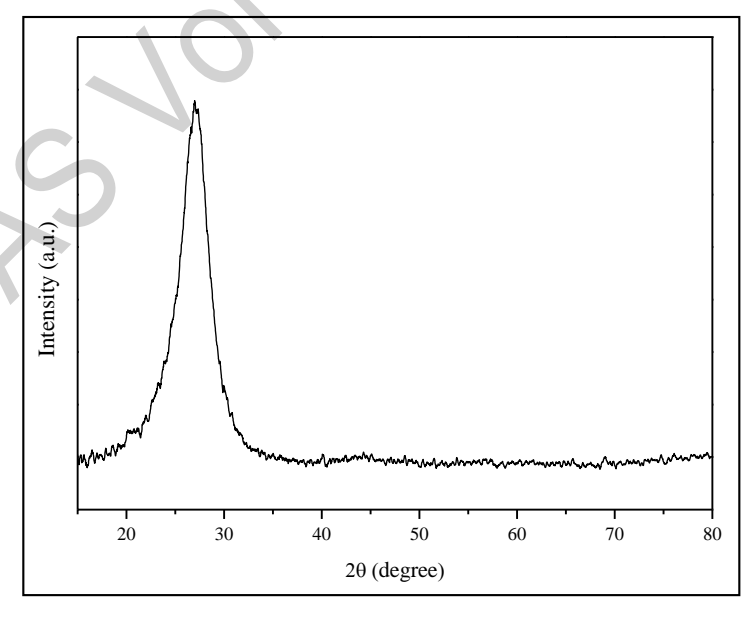


Figure 5. The XRD diffractogram of O-MCN

Table 1. The elemental analysis of O-MCN

| C (wt.%) | H (wt.%) | N (wt.%) | O (wt.%) |
|----------|----------|----------|----------|
| 37.43    | 2.30     | 49.38    | 10.89    |

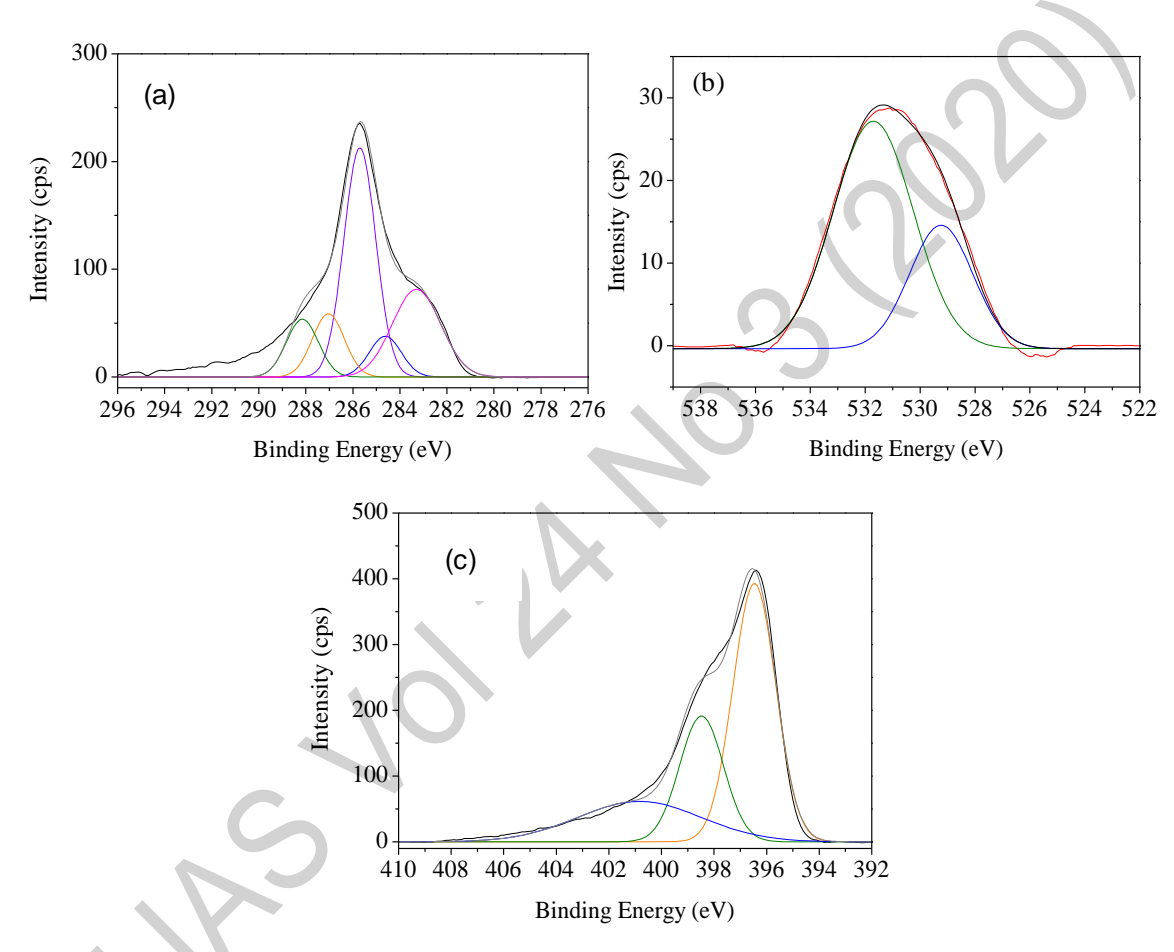


Figure 6. The XPS spectra for (a) C 1s, (b) O 1s, and (c) N 1s of -MCN

# UV-Vis diffuse reflectance analysis

The UV-Vis diffuse reflectance spectrum of O-MCN is shown in Figure 7(a). The catalyst exhibits intrinsic absorption in the ultraviolet region attributed to the band-band transition [28]. The absorption edge around 460 nm is as sociated with the photocatalytic property in the visible region [29, 30]. The bandgap energy ( $E_g$ ) of the composites was estimated from the intercept of a straight-line fitting to a plot of  $[F(R)hv]^{0.5}$  against hv

(Fig.7(b)), where F(R) is the Kubelka-Munk function and hv is the incident photon energy. From Figure 5(b), the calculated bandgap energy for O-MCN was 2.53 eV. The lower bandgap energy indicates that the O-MCN has potential to be used in photocatalys is under visible light irradiation.

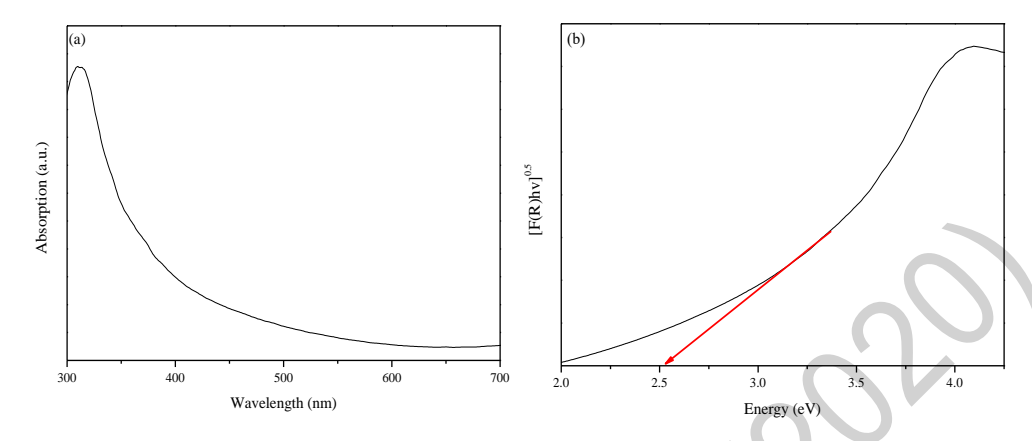


Figure 7. (a) The UV-Vis diffuse reflectance spectrum of O-MCN and (b) A plot of (F(R)hv) 0.5 vs photon energy

#### Conclusion

Oxygen doped mesoporous carbon nitride (O-MCN) with high purity was successfully synthesized via a hard-templating method. Urea and glucose were used as the carbon, oxygen and nitrogen source. The nanodisc silica (NDS) was used as a template. The O-MCN replicated the surface morphology of NDS; however, some changes were observed. The BET surface area of O-MCN (145 m<sup>2</sup>g<sup>-1</sup>) was slightly lower compared to NDS (152 m<sup>2</sup>g<sup>-1</sup>). The etching of NDS using aqueous HF had created pores with a broader diameter range (48- 84 Å) compared to NDS (39-203 Å). The UV–Vis diffuse reflectance analysis indicates that the O-MCN has the potential to be used in photocatalysis under irradiation. However, light visible investigations are needed to be carried out to understand the morphogenesis of the O-MCN since the HRTEM indicate morphological change after NDS removal.

#### Acknowledgement

The authors would like to thank the Malaysia Government for the following RU Grant (Grant No: 203/PKIMIA/6769001) and the TRGS grant (Ac. No. 203/PKIMIA/6769001), which partly supported this work. We would also like to thank TETFUND through the Federal Polytechnique Offa Kwara State, Nigeria for a scholarship to Shittu Fatimah Bukola.

#### References

- 1. Ajayan, S., Lakhi, K. S, Dae-Hwan, Al-Bahily, K. Cha, W. Viswanathan, B. and Choy, J. H. (2017). Mesoporous carbon nitrides: synthesis, functionalization, and applications. *Chemical Society Reviews*, 46: 72-101.
- 2. Luo, L., Zhang, A., Janik, M. J., Li, K., Song, C. and Guo, X. (2017). Facile fabrication of ordered mesoporous graphitic carbon nitride for RhB photocatalytic degradation. *Applied Surface Science*, 396: 78-84.
- 3. Lee, S. C., Lintang, H. O. and Yuliati, L. (2012). A urea precursor to synthesize carbon nitride with mesoporosity for enhanced activity in the photocatalytic removal of phenol. *Chemistry-An Asian Journal*, 7(9): 2139-2144.
- 4. Zhao, Z., Dai, Y., Lin, J. and Wang, G. (2014). Highly-ordered mesoporous carbon nitride with ultrahigh surface area and pore volume as a superior dehydrogenation catalyst. *Chemistry of Materials*, 26(10): 3151-3161.
- 5. Dong, G., Ai, Z. and Zhang, L. (2014). Efficient anoxic pollutant removal with oxygen functionalized graphitic carbon nitride under visible light. *RCS Advances*, 4: 5553-5560.

- Zhang, B., Li, X. J., Zhao, Y., Song, H. and Wang, H. (2019). Facile synthesis of oxygen doped mesoporous graphitic carbon nitride with high photocatalytic degradation efficiency under simulated solar irradiation. *Colloids and Surfaces:* A, 580: 123736.
- 7. Adam, F., Nelson, J. and Iqbal, A. (2012). The utilization of rice husk silica as a catalyst: Review and recent progress. *Catalysis Today*, 190(1): 2-14.
- 8. Lu, P. and Hsieh, Y. (2012). Highly pure amorphous silica nano-disks from rice straw. Powder Technology, 225: 149-155.
- Ghorbani, F., Sanati, A. M. and Maleki, M. (2015). Production of silica nanoparticles from rice husk as agricultural waste by environmental friendly technique. *Environmental Studies of Persian Gulf*, 2(1): 56-65.
- 10. Hu, J., Zhang, Z., Wang, F., Zheng, S., Cai, J., Qin, J., Liu, W., Liang, L. and Jiang, X (2016). A controllable synthesis of nitrogen-doped mesoporous carbon supported MoS<sub>2</sub> catalysts for hydrodesulfurization of thiophene. *RSC Advances*, 6(103): 101544-101551.
- 11. Deng, Q. F., Liu, L., Lin, X. Z., Du, G., Y Liu, Y. and Yuan, Z. Y. (2012). Synthesis and CO<sub>2</sub> capture properties of mesoporous carbon nitride materials. *Chemical Engineering Journal*, 203: 63-70.
- 12. Sung. S. P., Sang-Wook, C., Chunfeng, X., Dongyuan, Z., and Chang-Sik, H. (2011). Facile synthesis of mesoporous carbon nitrides using the incipient wetness method and the application as hydrogen adsorbent. *Journal of Materials Chemistry*, 21: 10801-10807.
- 13. Wangsoo, C., In, Y. K., Jang, M. L., Sungho, K., Kavitha, R., Kothandam, G., Selvarajan, P., Siva, U. and Ajayan, V. (2019). Sulfur-doped mesoporous carbon nitride with an ordered porous structure for sodium-ion batteries. *ACS Applied Materials & Interfaces*, 11: 27192-27199.
- Chang, S., Clair, B., Ruelle, J., Beauchêne, J., Renzo, F. D., Quignard, F., Zhao, G., Yamamoto, H. and Gril, J. (2009). Mesoporosity as a new parameter for understanding tension stress

- generation in trees. *Journal of Experimental Botany*, 60(11): 3023-3030.
- 15. Mousavi, M., Habibi-Yangjeh, A. and Abitorabi, M. (2016). Fabrication of novel magnetically separable nanocomposites using graphitic carbon nitride, silver phosphate and silver chloride and their applications in photocatalytic removal of different pollutants using visible-light irradiation. *Journal of Colloid and Interface Science*, 480: 218-231.
- Xu, H. Y., Wu, L. C., Zhao, H., Jin, L. G. and Qi, S. Y. (2015). Synergic effect between adsorption and photocatalysis of metal-free g-C<sub>3</sub>N<sub>4</sub> derived from different precursors. *PLoS One*, 10(11): 1-20.
- 17. Liu, J., Zhang, T., Wang, Z., Dawson, G. and Chen, W. (2011). Simple pyrolysis of urea into graphitic carbon nitride with recyclable adsorption and photocatalytic activity. *Journal of Material Chemistry*, 21(38): 14398-14401.
- 18. Guo, Q., Xie, Y., Wang, X., Zhang, S., Hou, T. and Lv, S. (2004). Synthesis of carbon nitride nanotubes with the  $C_3N_4$  stoichiometry via a benzene-thermal process at low temperatures. *Chemical Communications*, 1: 26-27.
- 19. Luo, J., Cui, Z. and Zang, G. (2013). Mesoporous metal-containing carbon nitrides for improved photocatalytic activities. *Journal of Chemistry*, 2013: 1-6.
- Muniandy, L., Adam, F., Rahman, A., Iqbal, A., Ruzaina, N. and Rahman, A. (2017). Applied surface science from melamine for the liquid phase hydroxylation of benzene and VOCs. *Applied Surface Science*, 398: 43-55.
- 21. Nghiem, L., Tuan, A., Thi, L., Dung, K., Doan, L. and Ha, T. (2017). Preparation and characterization of nanosilica from rice husk ash by chemical treatment combined with calcination. *Vietnam Journal of Chemistry*, 55(4): 455-459.
- 22. Kwon, K., Sa, Y. J., Cheon, J. Y. and Joo, S. H. (2012). Ordered mesoporous carbon nitrides with graphitic frameworks as metal-free, highly durable, methanol-tolerant oxygen reduction catalysts in an acidic medium. *Langmuir*, 28(1): 991-996.

- 23. Mitra, A., Howli, P., Sen, D., Das, B. and Chattopadhyay, K. K. (2016). Cu<sub>2</sub>O/g-C<sub>3</sub>N<sub>4</sub> nanocomposites: An insight into the band structure tuning and catalytic efficiencies. *Nanoscale*, 8(45): 19099-19109.
- 24. Chena, Z., Wua, Y., Wanga, Q., Wang, Z., Heb, L. Lei, Y. and Wang, Z. (2017). Oxygen-rich carbonnitrogen quantum dots as cocatalysts for enhanced photocatalytic H<sub>2</sub> production activity of TiO<sub>2</sub> nano fibers. *Progress in Natural Science: Materials International*, 27(3): 333-337.
- 25. Seredych, M. and Bandosz, T. J. (2016). Nitrogen enrichment of S-doped nanoporous carbon by g-C<sub>3</sub>N<sub>4</sub>: Insight into photosensitivity enhancement. *Carbon*, 107: 895-906.
- 26. Wei, F., Liu, Y., Zhao, H., Ren, X., Liu, J., Hasan, T., Chen, L., Li, Y. and Su, B. (2018). Oxygen selfdoped g-C<sub>3</sub>N<sub>4</sub> with tunable electronic band structure for unprecedentedly enhanced photocatalytic performance. *Nanoscale*, 4: 4515-4522.

- 27. Wang, K., Wang, X., Pan, H., Liu, Y., Xu, S. and Cao, S. (2018). In situ fabrication of CDs/g-C<sub>3</sub>N<sub>4</sub> hybrids with enhanced interface connection via calcination of the precursors for photocatalytic H<sub>2</sub> evolution. *International Journal of Hydrogen Energy*, 43(1): 91-99.
- 28. Kautz, A. C., Kunz, P. C., Janiak, C. and Kautz, A. C. (2016). CO-releasing molecule (CORM) conjugate systems. *Dalton Transactions*, 45(45): 18045-18063.
- 29. Li, J., Shen, B., Hong, Z. Lin, B. (2012). A facile approach to synthesize novel oxygen-doped g-C<sub>3</sub>N<sub>4</sub> with superior visible-light photoreactivity. *Chemical Communications*, 98(48): 12017-12019.
- 30. Bandosz, T. J. (2016). Nitrogen-doped activated carbon-based ammonia sensors: Effect of specific surface functional groups on carbon electronic properties. *ACS Sensors*, 1(5): 591-599.